ELSEVIER

Sedimentary Geology 143 (2001) 15–39

Sedimentary Geology

www.elsevier.com/locate/sedgeo

Early diagenetic stabilization of trace elements in reptile bone remains as an indicator of Maastrichtian–Late Paleocene climatic changes: evidence from the Naran Bulak locality, the Gobi Desert (South Mongolia)

V.S. Samoilov[a,*], Ch. Benjamini[a], E.V. Smirnova[b]

[a]*Department of Geological and Environmental Sciences, Ben-Gurion University of the Negev, Beer Sheva 84105, Israel.*
[b]*Vinogradov Institute of Geochemistry, Russian Academy of Sciences, Irkutsk 664033, Russia*

Received 5 August 1999; accepted 15 December 2000

Abstract

Maastrichtian dinosaur bone remains from the Naran Bulak locality (the Gobi Desert) with well-preserved bone textural features are enriched in some trace elements, primarily in REE. These features of vertebrate fossils were formed during diagenesis following rapid burial in mudflow sediments, and prior to postfossilization epigenetic changes. Trace elements are mainly concentrated in diagenetic apatite. Their contents in the bones correlate with that in their enclosing sediments for both maxima and minima. Fossil and sediment compositions were established under the influence of paleoclimate. They are correlated with long-term climatic changes with the aridity maximum at the K/T boundary. Climatic changes were recorded via the change of salinity of waters interacting with the buried vertebrate remains.

Keywords: K/T boundary; Dinosaur; Bone diagenesis; Geochemistry; South Mongolia

1. Introduction

Trace element geochemistry of faunal remains, primarily their REE enrichment, contains paleoenvironmental information. Postmortem geochemical changes in fish remains and ichthyoliths contribute to our understanding of faunal taphonomy and preservation (Kolodny, 1983; Kolodny and Luz, 1992; McArthur and Walsh, 19841985; Elderfield and Pagett, 1986; Wright et al., 1987; Grandjean et al., 1987, 1988, 1993; Schmitz et al., 1991; Wang and Cerling, 1994). The importance of bone apatite for study of these changes has been established (Luz and Kolodny, 1985, 1989; Wright et al., 1987; Newesley, 1989; Lee-Thorp and Vander Merwe, 1991; Grandjean and Albarede, 1993; Sanchez Chillon et al., 1994; Bryant et al., 1996; Person et al., 1996). In recent years, geochemical investigations have been extended to large terrestrial vertebrates, mainly to mammal remains. These investigations also indicate a relationship between geochemical features of terrestrial vertebrates and some biospheric events (Longinelli, 1984; Luz et al., 1984, 1990; Williams, 1988; Ayliffe et al., 1992; Bocherens et al., 1994; Bryant et al., 1994; Sillen and Lee-Thorp, 1994; Downing and Park, 1998).

Attention has been also paid to the geochemical

* Corresponding author. Fax: +972-7-6472997.
E-mail address: samoilov@bgumail.bgu.ac.il (V.S. Samoilov).

0037-0738/01/$ - see front matter
PII: S0037-0738(00)00192-5

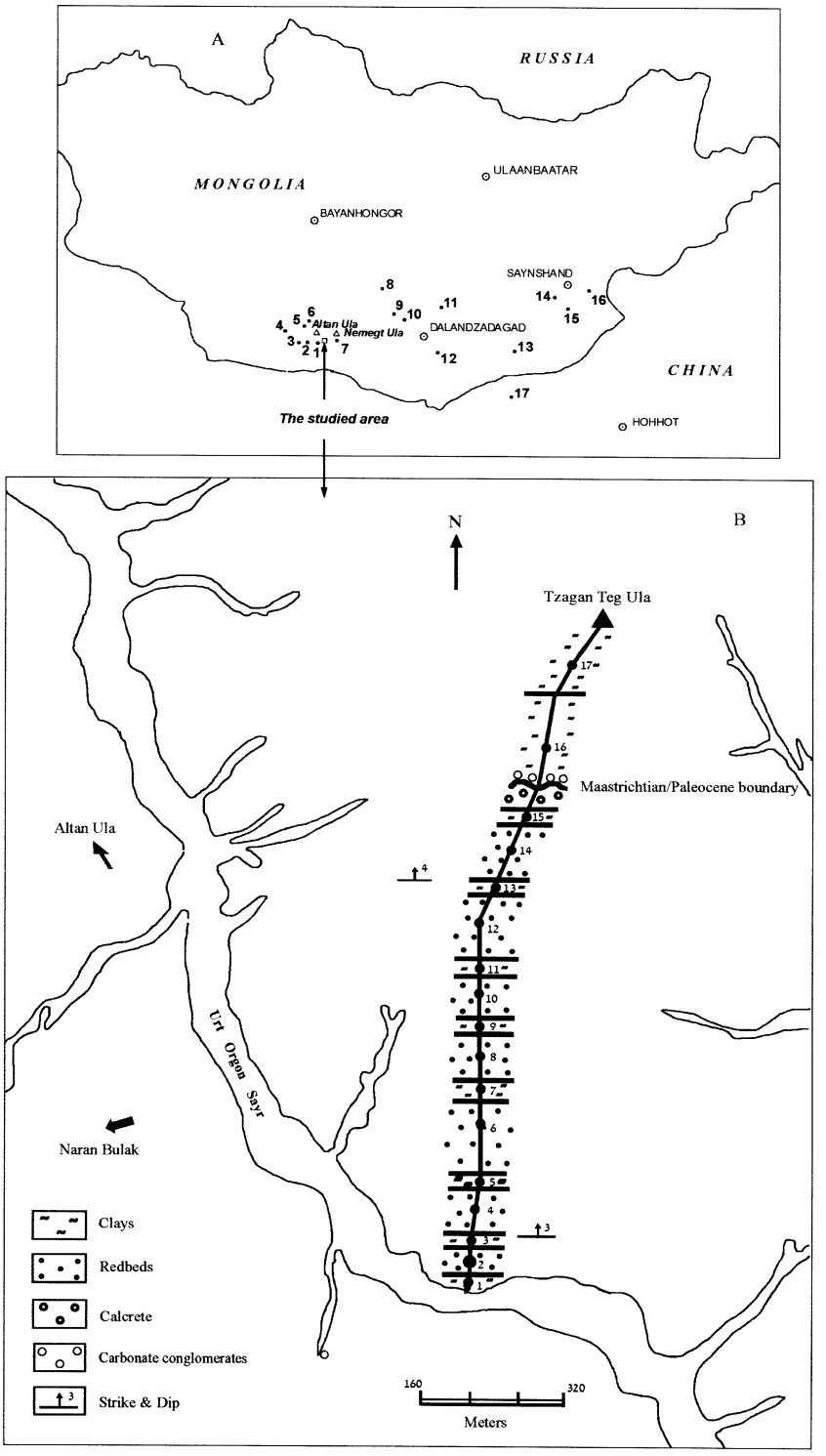
A
RUSSIA
MONGOLIA
ULAANBAATAR
BAYANHONGOR
SAYNSHAND
DALANDZADAGAD
Altan Ula
Nemegt Ula
The studied area
CHINA
HOHHOT
B
N
Tzagan Teg Ula
Maastrichtian/Paleocene boundary
Altan Ula
Urt Orgon Sayr
Naran Bulak
Clays
Redbeds
Calcrete
Carbonate conglomerates
Strike & Dip
160
320
Meters

study of dinosaur bone remains (Tauson et al., 1984, 1990, 1991; Barrick and Showers, 1994; Kolodny et al., 1996; Samoilov and Benjamini, 1996; Hubert et al., 1996; Trueman, 1996, 1999). This attention reflects the interest regarding dinosaur extinctions and biosphere events connected with the K/T boundary. Previous geochemical investigations of dinosaur remains revealed their relative enrichment in REE, Y, Sr, and Ba (Tauson et al., 1990, 1991; Samoilov and Benjamini, 1996; Trueman, 1996, 1999), which emphasizes the potential of these trace elements for the study of taphonomy, preservation, and some aspects of paleogeographical reconstruction near the close of the Cretaceous.

The Gobi Desert of Mongolia is known for its late Mesozoic localities of dinosaur remains (Rozhdestvensky and Tatarinov, 1964; Kielan-Jaworowska, 1969; Gradzinski et al., 1977; Barsbold, 1972; Shuvalov, 1982; Jerzykiewicz et al., 1993). Previous investigations (Tauson et al., 1984, 1990, 1991; Samoilov and Benjamini, 1996) were based on geochemical characteristics of a broad spectrum of dinosaur remains collected from different Cretaceous deposits of South Mongolia, dated from Berriasian to Maastrichtian. The present work examines trace element geochemistry of vertebrate fossil remains and enclosing sediments as possible indicators for the changes in paleoclimatic conditions during the Maastrichtian–Late Paleocene in the Gobi Desert. We focus here on samples collected from a single section of Maastrichtian–Late Paleocene deposits, from the Naran Bulak locality in the Transaltai Gobi (Fig. 1A), among the best localities for preservation of Maastrichtian dinosaur and other vertebrate remains in South Mongolia.

2. General geology

The end of the Cretaceous and the beginning of the Tertiary (~80 to 45 Ma) are characterized by a significant pause in geotectonic and magmatic processes in South Mongolia (Samoilov, 1989). During this time, accumulation of continental sediments predominated. The beginning and middle of the Late Cretaceous are characterized by the widespread occurrence of lake deposits, particularly in the Bayan Shire Formation (Cenomanian–Santonian). Primarily lacustrine sediments (calcareous sandstones, clays, and loams) with rare alluvial deposits (conglomerates and sandstones) comprise this formation, achieving a maximum thickness of 350 m in southeastern Gobi and a minimum of 70 m in Transaltai Gobi. The deposits of the Bayan Shire Formation are rich in dinosaur, other reptiles, and mollusk remains (Shuvalov, 1982; Devyatkin and Shuvalov, 1990).

Lacustrine sedimentation became sporadic in the Early Campanian and became restricted to small, intermittent lakes. The deposits of this time, assigned to the Djadokhta Formation, are represented mainly by eolian deposits (Jerzykiewicz et al., 1993). They were formed under a semiarid climatic regime, in an eolian-dominated environment of dune fields, small interdune ephemeral ponds, and streams. One important feature of the Djadokhta deposits was the formation of redbeds enriched in vertebrate remains as a result of sandstorm events. These were short-term, high-energy desert events and played a very important role in depositional environment and vertebrate burial (Jerzykiewicz et al., 1993).

Lacustrine sedimentation resumed an important role in the Middle–Late Campanian with the deposition of the Barun Goyot Formation (Shuvalov, 1982; Devyatkin and Shuvalov, 1990; Jerzykiewicz et al., 1993). The Barun Goyot Formation is composed primarily of lacustrine sandstones and clays, but eolian deposits present also in some regions (Jerzykiewicz, 1998). The Barun Goyot Formation is no more than 150 m thick, with a maximum in the western part of South Mongolia.

The character and scale of sedimentation changed again in the Maastrichtian. Lacustrine basins of this time were considerably reduced. Maastrichtian sediments are represented by of the Nemegt Formation,

Fig. 1. Location map of the studied area. A, Location map of Naran Bulak and some other Cretaceous dinosaur-bearing sites (black circles) in the Gobi Desert. 1, Naran Bulak; 2, Tsagan Khusu; 3, Khermeen Tsav; 4, Nogon Tsav; 5, Khaichin Ula; 6, Bugin Tsav; 7, Khulsan; 8, Toogreek; 9, Bayn Dzak; 10, Khashaat; 11, Tsogt Obo; 12, Tsulutu Ula; 13, Baynshin Tsav; 14, Khara Khutul; 15, Bayan Shire; 16, Khamrin Us; and 17, Bayan Mandahu. B, The studied sequence between Urt Orgon Sayr and Tsagan Teg Ula. Numeric labels indicate the bed numbers and the black circles indicate the sampling points (see Table 1). Based on aerial photograph positioning.

Table 1
Stratigraphic log, the Naran Bulak locality

Age	Formation	NN beds	Thickness (m)	Lithology	Description	Sampling[1*]		
						Remains		Sediments
						Dinosaur[2*]	Turtle[3*]	
Late Paleocene	Naran Bulak	18	12		Red clays with rare faunal remains		18T	18sed
		17	17		White clays with rare faunal remains		17T(M.)	17sed
		16	14		Grey clays bearing rare faunal remains with basal carbonate conglomerates		16T	16sed
Maastrichtian	Nemegt		2.5		Greyish carbonate caliche without faunal remains			
		15	9.3		Greyish-greenish clays without faunal remains			15sed
		14	1.8		Red sandstone with rare vertebrate remains	14E	14T	14sed
		13	9.4		Greyish-greenish clays with rare shelly fossils			13sed
		12	2.1		Red sandstone with abundant vertebrate remains	12V, 12E, 12S, 12P	12T	12sed
		11	8.9		Greyish-greenish clays with shelly fossils			11sed
		10	1.7		Red sandstone with abundant vertebrate remains	10V, 10E, 10AI	10T (M.)	10sed
		9	9.6		Greenish clays with shelly fossils			9sed
		8	1.3		Red sandstone with abundant vertebrate remains	8V, 8E, 8S, 8P, 8R	8T	8sed
		7	10.1		Greyish-greenish clays with shelly fossils			7sed
		6	0.5		Red sandstone with abundant vertebrate remains	6V, 6E, 6AI	6T	6sed
		5	11.2		Greenish clays with shelly fossils			5sed
		4	0.7		Red sandstone with abundant vertebrate remains	4V, 4E	4T	4sed
		3	9.7		Greyish-greenish clays with shelly fossils			3sed
		2	1.2		Red sandstone with abundant vertebrate remains	2V, 2E, 2S, 2R, 2AI	2T (M.)	2sed
		1	9.2		Greyish-greenish clays with shelly fossils			1sed
Campanian	Barun Goyot				Reddish clays with rare shelly fossils			

1*) Sample number, see Tables 2-6; 2*) V - vertebrae, E - extremities, S - skull, P - pelvis, R - ribs, AI - epigenetically altered remains;
3*) (M.) - the remains of turtle *Mongoleums*.

mainly noted in the Transaltai Gobi around the Nemegt Ridge (Naran Bulak, Tzagan Khushu, Bugyn Tsav and other regions) and partly in the northern and eastern part of the Gobi Desert (Shuvalov, 1982). Lacustrine stratified clay deposits with the remains of mollusks, ostracods, conchostracans, charophytes and turtles (Barsbold, 1972; Martinson, 1975) play a considerable role in the Maastrichtian sequence of Transaltai Gobi. Lacustrine clay beds up to 10–12 m thick alternate with redbeds of mudflow origin, mainly calcareous sandstones up to 2 m thick. These redbeds include numerous and diverse remains of dinosaurs and other reptiles. Occasionally, eolian deposits are found on the periphery of these Maastrichtian lake basins. Lithological-facial and paleontological data show that the Maastrichtian lakes were mainly characterized by shallow depths, elevated salinity, and shoaling coasts with a broad beach zone. Considerable vegetative cover including forests was typical for lake and river coasts, but away from them dry steppe-like landscapes prevailed (Shuvalov, 1982).

Late Paleocene sediments belonging to the Naran Bulak Formation disconformably overlie Maastrichtian deposits. Erosion of the Maastrichtian deposits and absence of Danian and Early Paleocene deposits is typical for the stratigraphic section in Mongolia across the K/T boundary (Devyatkin, 1981).

Paleocene deposits are again represented mainly by lacustrine sediments—clays, sandstones, loams, and rare conglomerates. They include in their lowermost parts basal conglomerates up to 2 m thick, with abundant redeposited fragments of pedogenic calcrete deposits, cemented by carbonate silt material. Remains of reptiles, mammals and mollusks have been observed in Paleocene sediments, but no dinosaur remains (Devyatkin, 1981).

In our study, material was taken from the Naran Bulak Formation of the Maastrichtian, from its type region. The Naran Bulak region is situated in the Nemegt depression that separates the Nemegt and Tost-Noen ridges. This depression is composed of Mesozoic, Cenozoic and Quaternary sediments. Upper Cretaceous deposits occupy its northern part to the foot of Nemegt ridge. Today, this region is a desert characterized by badland landscape with cliffs, steep-sided gullies, small canyons and buttes. Rugged, steep hills with flat tops cutting through numerous ephemeral stream channels ('sayrs') are typical for this landscape. Laterally continuous, widespread exposures of the Maastrichtian strata occur in the walls of these sayrs.

The studied area lies about 6 km northeast of the Naran Bulak spring, where the complete stratigraphic section of the Maastrichtian deposits is exposed. This section begins at the bottom of Urt Orgon Sayr (Canyon), where Maastrichtian clays overlying the Barun Goyot Formation crop out northeastwards up to Tsagan Teg Ula (Fig. 1B).

Lacustrine clay deposits alternating with calcareous sandstone redbeds (Fig. 1B; Table 1) form most of the Maastrichtian section, up to 120 m thick. As a rule, redbeds are exposed in the gentle parts of the slopes. The thickness of the lacustrine beds ranges from 8.9 to 11.2 m, whereas the redbeds are only 0.5–2.1 m thick. However, faunal remains were mainly buried in the redbeds, and are considerably rarer in the lacustrine deposits.

At Tsagan Teg Ula, the lower and middle parts of the Paleocene Naran Bulak Formation overlie the deposits of Nemegt Formation. The upper part of Naran Bulak Formation was observed to the east of the Tsagan Teg Ula at Ulan Bulak (Devyatkin, 1981).

3. Maastrichtian sedimentary facies

Three groups of Maastrichtian deposits, differing by lithological and formation features, are distinguished in the studied sequence: (1) lacustrine deposits; (2) mudflow deposits; and (3) pedogenic deposits.

Large-scale, concordant, horizontally bedded strata up to 11 m thick represent the lacustrine deposits. The thickness of these deposits varies (Fig. 2), with the maximum (11.2 m) for bed N5 of the lower sequence and the minimum for bed N1 (9.2 m) and bed N15 (9.3 m). These strata, as a rule, are thin bedded and laminated, and individual interbeds, 0.2–13 cm thick, are easily traced along the strike. Cross bedding is absent.

Considerable variation of thickness of interbeds is noted. Thin laminations with silt–shale interbeds up to 2–3 cm thick prevail, but are usually combined with thicker sandy–silty–clay interbeds up to 13 cm thick observed in the upper part of the studied sequence. This pattern shows that: (a) sedimentation

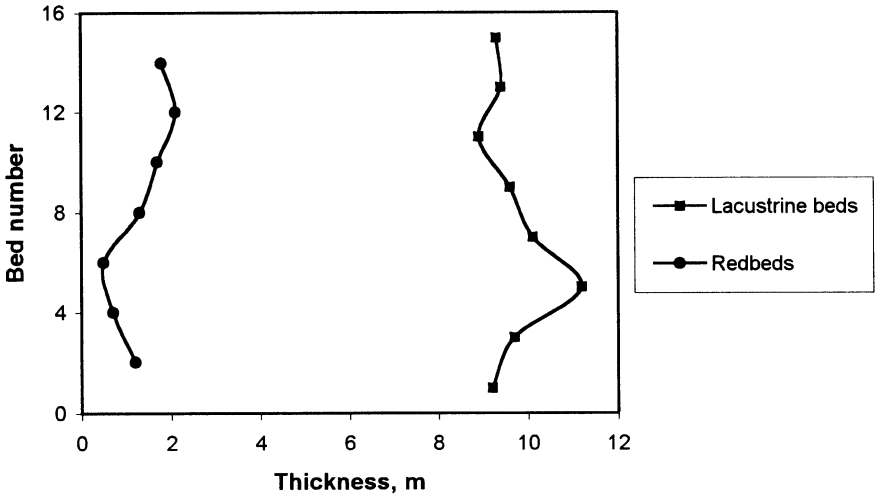

Fig. 2. Thickness variations of Maastrichtian beds in the studied sequence.

in calm waters was periodically disturbed by the introduction of storm beds charged with sand; and (b) the lacustrine beds of the upper sequence were formed in a more shallow setting.

The studied lacustrine sediments are mainly silty-shaley with rare sand fraction. Clay content ranges from 20% in the thickest interbed to 65% in the thinnest interbed, while silt rises with the increase in interbed thickness from 30 to 60%. The thickest interbeds (up to 13 cm) are characterized by up to 20% sand.

The lacustrine sediments are light colored and are greenish-grayish or yellow-grayish. They are mainly composed of clay minerals and quartz, with minor feldspar, calcite, and gypsum and small amounts of dolomite, pyrite, chlorite, and sericite. Montmorillonite and kaolinite are represented in the clay fraction. Chemical analyses of the lacustrine sediments (Table 2) indicate that authigenic mineral content increases towards the K/T boundary, while a concentration minimum is noted for lacustrine bed N5.

Shelly fossils are more abundant in the lower and middle lacustrine beds, rare in the upper lacustrine beds, and were not found in the uppermost lacustrine bed. Their generally good preservation indicates burial in a low-energy setting.

Carbonate-rich sandstones of horizontal redbeds up to 2.1 m thick represent mudflow sediments. The thickness of these mudflow deposits varies (Fig. 2) with the minimum for redbed N6 (0.5 m) and with the maximum for the uppermost redbeds, N12 and 14 (1.8 and 2.1 m). They are not internally stratified, and lack lamination or cross bedding. The redbed matrix is formed by inequigranular, fine- to medium-grained sand with silt (up to 30%) and clay (up to 15%). The sand is mainly formed by quartz and feldspar with minor light mica, limonite, calcite, and gypsum.

Mottled structure and conglomerate texture characterize redbeds owing to the presence of light carbonate-rich mottles in red or reddish sandstone matrix (termed 'pseudoconglomerates' in the Russian and Mongolian studies). The amount of carbonate mottles is minimal in the lower part (bed N6) and increases in the uppermost bed (N14). These mottles are irregular, lenticular to rounded, ranging from sub-cm up to 10–15 cm in diameter. They are mainly composed of carbonate, but gypsum, dolomite, halite, quartz, feldspar, and clay minerals are also present. As contacts between carbonate-rich mottles and enclosing sandy matrix are usually clear and sharp, we believe that they represent allochthonous pebbles within a red sandstone matrix. Carbonate-rich inclusions in redbeds are fragments of calcrete pedogenic deposits broken up by the mudflows and reburied in sandy material during severe rainstorm events typical for desert regions.

Pedogenic calcrete deposits are observed in situ in

Table 2
Contents of some major (wt%) and trace elements (ppm) in Maastrichtian–Late Paleocene sediments of the Naran Bulak locality. (Bed numbers increase from the base upwards, see Table 1)

	CaO	CO_2	P_2O_5	SO_3	Cl	Sr	Ba	La	Ce	Nd	Yb	Y	Sr/Ba	La/Yb
18	3.07	1.87	0.08	0.70	0.11	165	125	32	55	30	1.6	19	1.32	20
17	4.35	2.56	0.09	0.73	0.21	220	180	39	69	30	1.8	25	1.22	22
16	6.58	4.13	0.08	1.50	1.05	380	380	50	95	36	2.1	32	1.00	24
15	8.31	5.32	0.09	2.02	1.77	430	450	69	135	50	2.1	45	0.96	33
13	6.80	4.41	0.08	1.77	1.55	410	430	65	120	50	2.1	45	0.95	31
11	6.61	4.23	0.10	1.75	1.11	410	350	64	120	50	2.1	40	1.17	30
9	5.60	3.66	0.09	1.31	0.73	320	285	60	110	45	2.0	39	1.12	30
7	4.85	3.05	0.08	1.25	0.25	280	240	58	115	42	2.0	36	1.04	29
5	3.72	2.29	0.08	0.82	0.30	250	235	50	78	40	2.0	32	1.19	25
3	6.16	3.96	0.11	1.45	0.45	350	260	45	83	38	2.0	31	1.35	23
1	6.64	3.99	0.09	2.00	0.62	330	260	45	88	37	2.1	32	1.27	21
14	20.58	14.71	0.17	2.38	1.49	420	450	63	120	50	2.1	47	0.93	30
12	19.50	14.14	0.15	2.26	1.34	420	440	65	122	50	2.1	45	0.95	31
10	17.36	12.08	0.18	2.40	0.78	395	380	65	120	45	2.0	40	1.04	33
8	15.51	10.90	0.19	1.74	0.81	330	300	58	110	45	2.1	38	1.10	28
6	10.36	7.29	0.17	1.09	0.44	280	250	49	75	40	2.0	30	1.12	25
4	13.04	9.15	0.18	1.50	0.59	320	300	44	80	36	2.0	31	1.07	22
2	16.77	11.63	0.16	2.12	0.73	350	310	48	96	35	2.1	34	1.13	23

the uppermost part of the Maastrichtian sequence, where one reasonably indurated calcrete bed overlies the uppermost lacustrine bed (Fig. 1B; Table 1). Late Paleocene deposits overlie them, following erosion and unconformity. The thickness of pedogenic deposits varies considerably along the strike and ranges up to 2.5 m. The calcretes are light, grayish carbonate rocks without internal stratification. They contain typical rhizocretions with cone-shaped hollows filled with sand, but faunal remains are absent.

The noted relict of calcrete profile corresponds to a mature stage of calcrete pedogenesis with the development of a continuous carbonate horizon (Gile et al., 1981). Identical paleosol horizons formed in the Campanian are known from the southeastern part of the Gobi Basin (Jerzykiewicz et al., 1993). They were apparently common in the hinterland of the lacustrine deposits and contributed to mudflow sediments.

4. Facial and taphonomic features of vertebrate fossil occurrence

In the studied area, Maastrichtian faunal remains are almost entirely restricted to redbed lithofacies. This close relationship suggests a close link between vertebrate fossils and the processes of the formation of the enclosing sediments.

Dinosaur remains belong mainly to medium- and small-size individuals. Associated, articulated, and partly articulated skeletons are typical. As a rule, they did not suffer considerable mechanical wear, indicating rapid burial. However, fragments of disarticulated skeletons are presented as well. These rarer fragments are frequently characterized by considerable mechanical wear, evidence of a lengthy interval of exposure between the dinosaur death and bone burial.

Dinosaur bone remains are usually subhorizontally oriented. In spite of the rich assemblage of vertebrate bone remains, coprolites, burrows, dinosaur and other reptile fossil eggs or their fragments are absent. As these are common elsewhere in the Gobi Desert deposits, apparently the process of redbed formation was not compatible with their preservation.

Our taphonomic interpretation of most of faunal remains is that in the course of severe desert rainstorm events, live animals were entrapped and buried within mud- and debris flows. Thus, in most cases buried vertebrates were encased within the redbeds simultaneously with their deposition, corresponding to their time of death. However, some bones lying about on the surface were incorporated as well. This explains the association of articulated and disarticulated

Table 3
Chemical composition of bone fossil forming minerals

Component	Apatite[a]				Calcite					
	2E	8E	12E	8sed	2E	8E	12E	2Al	8Al	12Al
SiO_2(%)	1.56	1.50	1.92	0.11	0.06	0.04	tr.	0.10	0.07	0.13
Al_2O_3 (%)	0.25	0.20	0.26	0.09	tr.	0.01	tr.	tr.	0.01	0.01
Fe_2O_3 (%)	tr.	0.11	tr.	0.11	0.26	0.08	0.12	0.52	0.28	0.21
FeO (%)	0.76	0.82	1.05	0.39	0.41	0.46	0.32	1.15	1.46	1.90
MnO (%)	0.20	0.28	0.23	0.16	0.27	0.11	0.15	0.33	0.54	0.38
MgO (%)	0.33	0.53	0.44	0.22	0.33	0.24	0.13	0.69	0.99	1.04
CaO (%)	52.12	51.86	51.88	53.30	54.69	54.36	55.00	52.08	52.41	52.20
Na_2O (%)	1.17	1.37	1.46	0.33	0.29	0.15	0.21	0.12	0.08	0.11
K_2O (%)	0.15	0.11	0.15	0.02	0.01	tr.	tr.	0.03	0.01	tr.
P_2O_5 (%)	33.71	32.72	31.82	41.39	nd	nd	nd	nd	nd	nd
CO_2 (%)	3.25	4.31	4.29		43.38	43.20	43.68	43.76	43.22	43.50
SO_3 (%)	2.21	2.16	2.30	0.18	0.06	tr.	0.10	0.03	0.01	tr.
F (%)	3.31	3.62	3.83	3.45	nd	nd	nd	nd	nd	nd
Cl (%)	tr.	0.02	tr.	tr.	nd	nd	nd	nd	nd	nd
H_2O^+ (%)	1.18	0.90	0.87	0.24	nd	nd	nd	nd	nd	nd
H_2O^- (%)	0.45	0.25	0.21	0.12	0.46	0.54	0.37	0.55	0.39	0.63
O = F,Cl (%)	1.39	1.52	1.61	1.45						
Total (%)	99.26	99.24	99.10	100.11	100.22	99.19	100.08	99.36	99.47	100.11
Number of ions in formulaa										
Element										
Ca	9.31	9.21	9.17	9.73	0.99	0.99	0.99	0.93	0.96	0.94
Na	0.38	0.44	0.47	0.11	0.009	0.005	0.007	0.004	0.004	0.004
K	0.03	0.02	0.03							
Fe^{3+}		0.01		0.01	0.003	0.001	0.002	0.007	0.004	0.003
Fe^{2+}	0.11	0.11	0.14	0.05	0.001	0.001		0.002	0.002	0.003
Mn	0.03	0.04	0.03	0.02						
Mg	0.08	0.13	0.11	0.00	0.001	0.001	0.001	0.002	0.002	0.003
Al	0.05	0.04	0.05	0.02						
P	4.76	4.58	4.44	5.96						
C	0.74	0.97	0.97		1.00	1.00	1.00	1.00	1.00	1.00
Si	0.26	0.25	0.32	0.02						
S	0.28	0.27	0.29	0.02						
F	1.74	1.91	2.00	1.86						
Cl		0.01								
OH	0.66	0.50	0.47	0.13						
Trace elements (ppm)										
Sr	2540	3100	3360	840	1350	1600	1780	280	240	200
Ba	950	1100	1180	650	540	650	690	950	820	1380
Pb	150	166	170	48	56	71	88	22	45	33
Y	2900	3050	3200	195	140	165	180	20	12	10
La	1640	1850	2000	210	320	410	505	25	18	39
Ce	3050	3280	3200	340	700	730	780	38	25	50
Nd	1780	1700	1600	220	410	420	490	27	20	32
Sm	550	590	680	38	75	75	89	5.2	3.7	6.1
Gd	320	370	430	18	39	38	43	9.4	7.2	8.8
Dy	520	630	685	11	30	35	40	6.9	5.4	7.1
Yb	95	113	120	3.1	5.8	7.1	7.4	1.8	1.3	1.5

[a] For apatite, the number of ions was calculated on the basis 10(Ca, Mg, Fe, Mn, Al, Na, K).
tr. = traces.
nd = not determined.

skeletons, and the presence of bone remains both with and without mechanical wear.

5. Methods and materials

The sedimentary rocks associated with the Maastrichtian–Late Paleocene reptile remains were sampled (Fig. 1B; Table 1) for study of their lithological, mineralogical and geochemical features. Dinosaur bone remains (25 samples) were collected from Maastrichtian sediments, from the lower contact with the Barun Goyot Formation up to the pedogenic calcrete horizon beneath the Paleocene sediments. These samples represent different skeleton parts—vertebrae, extremities (phalangeal and basidigital bones), ribs, skull, and pelvis. These skeleton parts belonged to medium-size associated, articulated, or partly articulated skeletons, and only those devoid of significant mechanical wear were used. The remains of turtle carapace (10 samples) were sampled both from Maastrichtian redbeds and from later Paleocene beds. The turtle remains belonged partly to one genus, *Mongoleums*, whose range extends across the K/T boundary (Devyatkin, 1981). The position of the collected samples is shown in Fig. 1B and Table 1.

The dinosaur bone and turtle carapace remains are characterized by good external preservation. The dinosaur remains are mostly unaltered by epigenetic alteration that affects the interior parts of the skeletal remains more than their exterior. For best results, exterior, cortical or epiphyseal parts of slightly altered or unaltered bone remains were preferentially investigated. These parts were separated from the remaining bones and flushed out with distilled water to eliminate contamination of sand, clay, and hydrous ferric oxide. As established by point counting in thin sections, the samples chosen for analytical study were characterized by a relatively close relationship of phosphate and carbonate fractions (76–84% of apatite). This is the basis for the comparative geochemical study of the studied samples.

Analytical study of the faunal remains and sedimentary rocks was carried out in the Vinogradov Institute of Geochemistry, Academy of Science of USSR (Irkutsk, Russia). Optical emission spectrometry was the analytical method for REE and Y. This method and atomic absorption spectroscopy method were used for Sr, Ba, and Pb analysis. Chemical whole rock analysis was the method for major elements in sediments and faunal remains. For optical emission spectrometry, studied samples were diluted 10× using an artificial granite free from REE, and analyzed using the DFS-13 diffraction spectrograph. Standards for the analysis were SG-3 or SGD-1A. The lowest limits of the detection for REE in this analysis were (ppm): La, 10; Ce, 30; Nd, 10; Sm, 10; Gd, 10; Dy, 10; Yb, 1; and Y, 1. Other data on the analytical methods, including error bars, are given in previous publications (Samoilov and Kovalenko, 1993; Samoilov, 1984).

The analytical data correlate well with previous data on chemical composition of Maastrichtian bone remains and enclosing sediments from South Mongolia, showing similar tendencies in chemical change leading up to the K/T boundary (Tauson et al., 1991; Samoilov and Benjamini, 1996).

6. Results

6.1. The main geochemical features of the enclosing sedimentary rocks

Lacustrine and mudflow sediments may be distinguished on the basis of major element chemistry. Lacustrine sediments contain (wt%) only 3.7–8.3% CaO and 2.5–5.3% CO_2 with 0.8–2.0% SO_3 and 0.25–1.77% Cl with the maximum contents of these components in bed N15 from the uppermost part of the Maastrichtian section (Table 2). Calcareous sandstones forming the redbeds are enriched in calcite and, accordingly, are richer in CaO (up to 20.6%) and CO_2 (up to 14.7%) than lacustrine sediments. Mudflow sediments also contain gypsum (up to 5–6%) and sometimes halite, contributing up to 2.4% SO_3 and 1.5% Cl.

Apatite from redbeds is represented by the fluorine variety, poor in hydroxyl with F/OH = 14. This apatite is considerably depleted in Sr, Ba, Pb, Y, and REE relative to bone apatite. The REE spectrum of these phosphate fractions is also different (Table 3).

The lacustrine and mudflow sediments are similar in their high–low–high pattern of trace element distribution (Table 2; Fig. 3). The first maximum is found at the base of the Maastrichtian section (beds NN1 and 2). Trace element contents fall towards beds N6 and N7 and rise again towards the top of the Maastrichtian

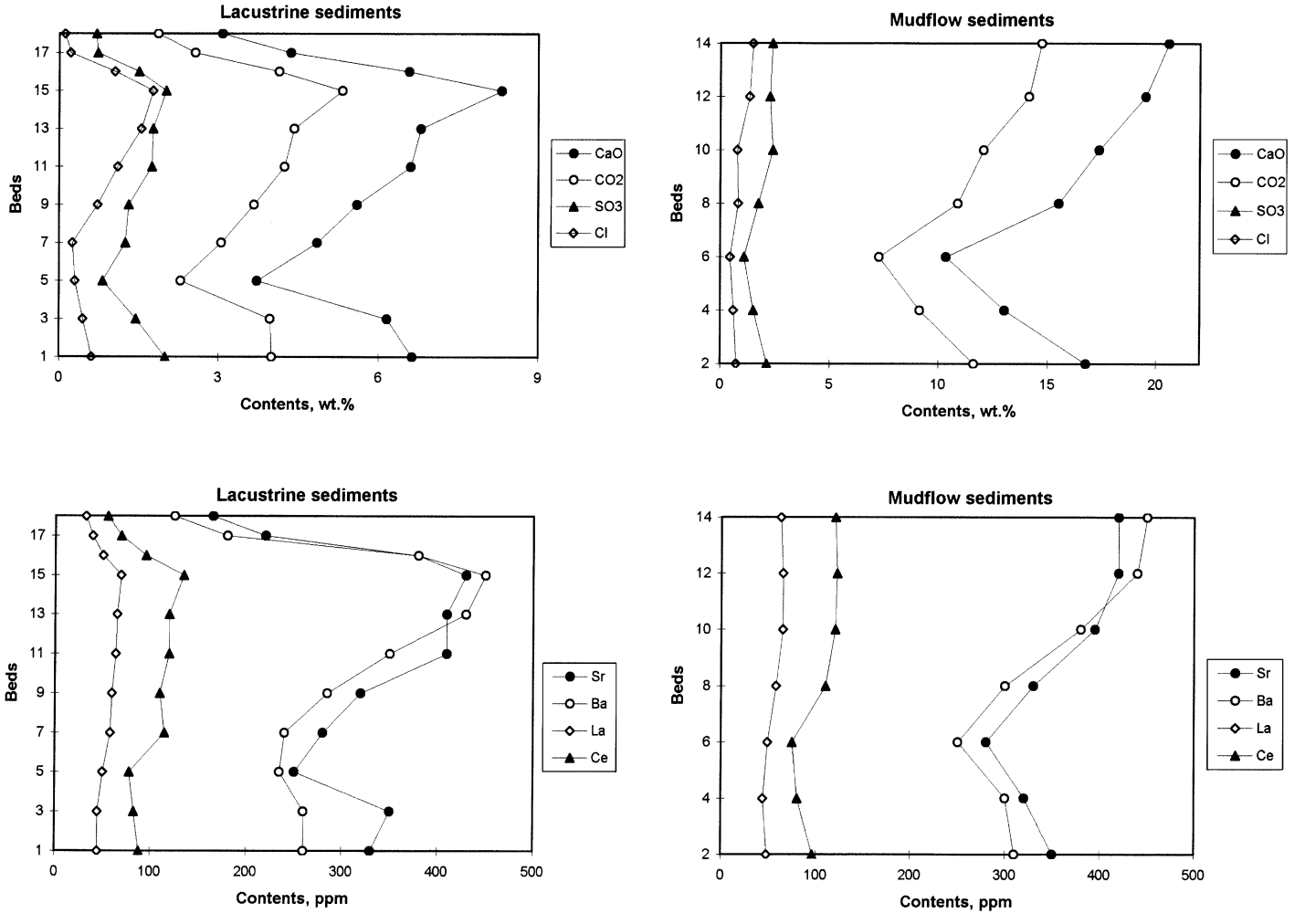

Fig. 3. Variations of sediment chemical composition in the studied sequence.

section, near the K/T boundary (beds N14 and N15). Concentrations decrease again for Paleocene lacustrine sediments from bed N16 to bed N18. An identical distribution pattern is observed for CaO, CO_2, SO_3, and Cl. Consequently, the distribution of rock-forming components and trace elements is characterized by a similar oscillating pattern with the same position of concentration maxima and minima.

The observed positive correlation between the contents of REE, Sr, and Ba, on the one hand, and CaO and CO_2, on the other hand (see Fig. 3), point to calcite as a sink for these trace elements. The rock enrichment in calcite is accompanied by the accumulation of the considered trace elements. Accordingly, the trace element maxima correspond to the maxima of calcite content both for lacustrine sediments and mudflow redbeds.

The value of the Sr/Ba ratio decreases slightly towards the top of the Maastrichtian. Sr/Ba $>$ 1 for the sediments of the lower and middle parts of the Maastrichtian section, while the upper part is characterized by Sr/Ba $<$ 1. The value of the La/Yb ratio increases towards the top of the section from 21 to 23 up to 30–33. A similar tendency is noted in distribution of La, Nd, and Y. The sediments of the uppermost part of the Maastrichtian deposits are especially enriched in these elements.

The tendency in the accumulation of trace elements clearly changes in the Paleocene. Late Paleocene sediments are distinguished by both sharply decreased concentrations of REE, Y, Sr, and Ba and their decrease upwards from the contact with Maastrichtian deposits. The lowest contents of trace elements are found in the uppermost Paleocene sediments. This is also noted for La/Yb ratio; on the contrary, Sr/Ba increases and is more than 1 (Table 2).

6.2. Petrographic and mineralogical features of bone remains

6.2.1. Dinosaur remains unaffected by late epigenetic processes

Dinosaur bone remains unaffected by epigenetic processes are mainly composed of two minerals,

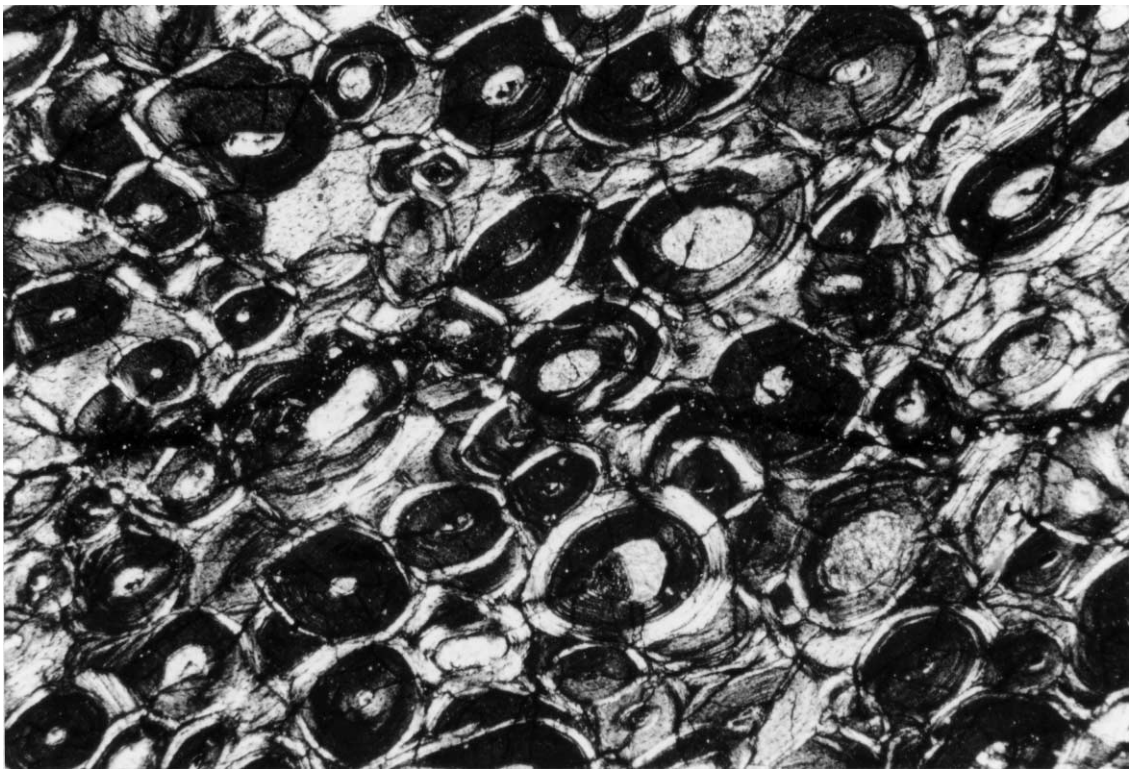

Fig. 4. Concentric texture of dinosaur bone fossils. Several osteons clearly show reversal lines, indicating that they were originally Haversian systems (Hubert et al., 1996).

apatite and calcite, and are characterized by concentric texture (Fig. 4) that equates to bone osteons (Hubert et al., 1996). Banded texture is occasionally observed at the border of the extremities. The bone remains with concentric texture contain abundant rounded calcite–apatite aggregates, from 0.05 to 6.0 mm in diameter, with a calcite core (nucleus) surrounded by apatite rim composed of regular concentric apatite laminae. The concentric structures are smaller in external bone parts (usually $d = 0.1$–0.2 mm here) and are larger (up to 6 mm) in internal bone parts. The diameter of the rounded calcite cores ranges from 0.01 mm at the exterior bone edge up to 4–5 mm in internal bone parts. Calcite nuclei are formed by a single calcite grain (crystal) in external bone parts, whereas they are composed of aggregated isometric calcite grains in internal bone material. These aggregates comprise from two to eight grains with diameter 0.2–1.5 mm. In oblique section, calcite aggregates are elongated.

Calcite content in bone remains varies. Bone cortex may contain 2–5% of calcite, whereas central bone parts (corresponding to originally spongy bone) consist of up to 70–80% of calcite. Accordingly, the apatite content in concentric structures increases towards the extreme exterior bone part, where bone is practically monomineralic, containing 95–98% apatite, with rare small calcite grains and hydrogoethite interbeds. The extreme exterior bone part with banded texture is characterized by the linear orientation of elongated thin apatite crystals parallel to the bone border.

The external parts of concentric structures are formed by aggregates of thinly laminated apatite crystals usually less than 0.001 mm wide and 0.15 mm long. These concentric zoned aggregates surround calcite centers (Fig. 5). The boundary between the apatite and calcite nucleus is sharp. The presence of black isotropic hydrogoethite (1–2%) is common in dinosaur bone remains. The hydrogoethite interbeds

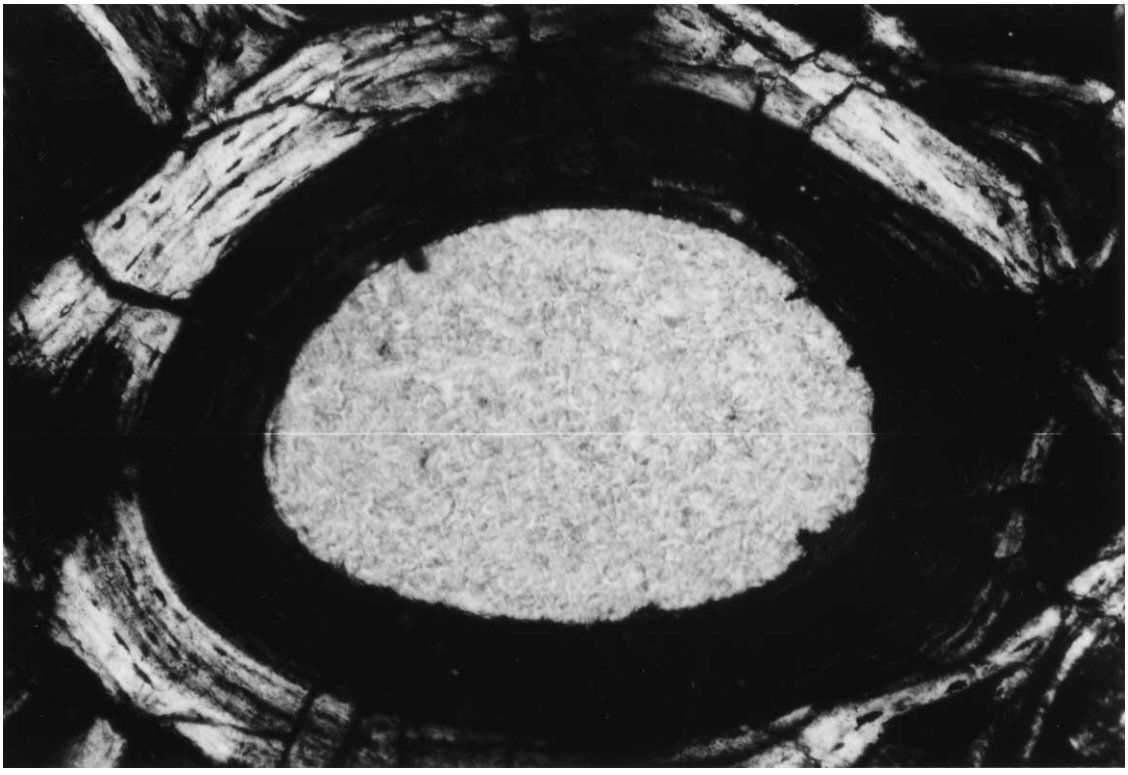

Fig. 5. The structure of individual calcite–francolite aggregate. Calcite nucleus (white), surrounded by thin platy crystals of francolite (black and white with black laminae). These crystals are much larger than original osteonic apatite and represent neoformed pseudomorphs.

(<0.004 mm long) are found also in bone apatite. These elongated crystals are usually oriented parallel to the apatite interbed.

The size of apatite crystals increases in the areas of their epigenetic recrystallization, usually along cracks, where apatite crystals range up to 0.01 mm wide and 1.2 mm long.

The apatite of the bone remains is represented by francolite, enriched in sulfur, silica, sodium, and some trace elements (Table 3). Fluorine content is 1.53–2.00 and OH content is 0.47–0.60 in the standard apatite formula, calculated on the basis of 10 cations for the Ca group (Deer et al., 1965). The value of the F/OH ratio varies in formula from 2.32 to 4.26 with 3.25–4.31% CO_2. Varieties richer in F are also richer in CO_2. The enrichment of apatite in phosphorus is accompanied by its depletion in C and F. Bone apatite contains 1.2–1.5% Na_2O or 0.4–0.5 in standard apatite formula (Table 3). Carbon, silica, and sulfur play a significant role in the anion group. The values of P/(C + Si + S) = 2.8–3.1 and C/(Si + S) = 1.4–1.6.

Bone apatite is rich in REE, as well as in Sr, Y, Ba, and Pb (Table 2). REE content is 0.80–0.87 wt% with the significant predominance of LREE. The value of the LREE/HREE ratio is 6.1–7.5 with La/Yb = 16–17. For the REE spectrum is typical Gd < Dy (Gd/Dy ~ 0.6). Bone apatite is characterized by Y ~ Ce and Y > La, Nd; it contains also 0.25–0.34% Sr and 0.10–0.12% Ba with Sr/Ba = 2.7–2.8.

On the whole, bone apatite from earlier Maastrichtian sediments is richest in P and OH but is most depleted in carbon, silica, sulfur, and alkalis. A minimum of F/OH and a maximum of P/(C + Si + S) also characterize this apatite. Apatite from later Maastrichtian sediments is richest in REE, Sr, Ba, Pb, and HREE relative to LREE.

Diagenetic calcite of calcite–apatite aggregates contains insignificant admixtures of Fe, Mg, and Mn, with 0.16–0.20% REE (about five times less than in early diagenetic bone apatite). LREE prevail with LREE/HREE = 20–21 and La/Yb = 55–68. In contrast to apatite, diagenetic calcite is characterized

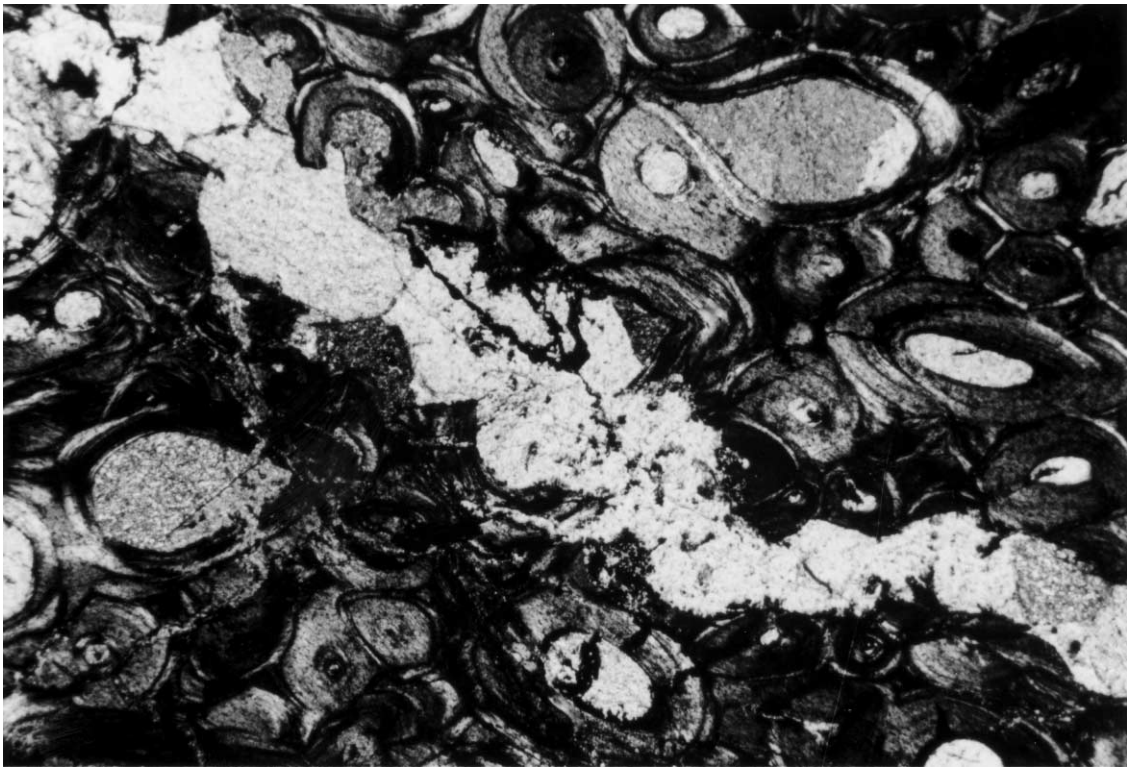

Fig. 6. Epigenetic calcite vein (white) in dinosaur bone fossil showing concentric texture.

by Gd > Dy (with Gd/Dy = 1.1–1.3) and Ce > La, Nd > Y. This calcite contains also less Sr—0.14–0.18% with Sr/Ba = 2.5–2.6.

Like apatite, diagenetic bone calcite is enriched in REE, Y, Sr, Ba, and Pb towards the K/T boundary. This is accompanied by an insignificant increase in the values of the LREE/HREE ratio (Table 3).

6.2.2. Epigenetically altered bone remains

The occurrence of epigenetic calcitization was one of the mineralogical–petrographical features of the bone remains. This process was more prominent in internal bone parts bordering with the porous bone center that corresponded to original spongy bone. Such open structure was favorable for the penetration of epigenetic solutions and for corresponding metasomatic changes of diagenetically fossilized bones. Epigenetic processes took place primarily within calcite nuclei with the recrystallization of early diagenetic calcite or with the development of secondary calcite veins up to 1.5–2.0 cm thick (Fig. 6). Epigenetic clay, barite, limonite, chalcedony and feldspar that are associated with the epigenetic calcite maybe simultaneous or later than the epigenetic calcitization. Epigenetic barite usually forms in parallel with calcite, but may also be later.

Epigenetic processes were accompanied by solution of bone apatite and led to the destruction of concentric bone texture. Epigenetic calcite forms fine-grained aggregates, ranging from 0.1 to 1.5 mm in diameter. The size of individual crystals is usually less than 0.02 mm, down to 0.005–0.006 mm.

Epigenetic calcite is geochemically distinguishable from early diagenetic calcite. This variety is richer in Fe, Mn, Mg, Ba (by 1.5–2.0 times), but is depleted in REE, Sr and Pb. Epigenetic calcite contains only 80–145 ppm of REE with Ce > La ~ Nd Gd Dy Sm Gd > Dy > Sm and is richer in HREE relative to LREE (LREE/HREE = 4.8–7.3 with La/Yb = 14–26). In addition, it contains only 200–280 ppm of Sr with 820–1380 ppm of Ba and is significantly distinguished from diagenetic calcite by its low value of the Sr/Ba ratio (0.1–0.3) (Table 3).

6.3. Main geochemical features of dinosaur bone remains

6.3.1. Dinosaur remains unaffected by late epigenetic processes

Unaltered dinosaur bone remains are mainly characterized by calcium carbonate–phosphate composition (Table 4). Silica, alkalis, iron and some volatiles (fluorine, sulfur, and water) play also an important role in their composition. Vertebrae, extremities, skull, pelvis and ribs are similar in whole fossil bone composition. Distinctions are noted between

Table 4
Chemical composition (wt%) of dinosaur bone remains (cortical and epyphyseal parts)

	Vertebrae			Extremities			Skull	Pelvis	Ribs	Altered extremities		
	2V	8V	12V	2E	8E	12E	8S	8P	8R	2Al	8Al	12Al
SiO_2	2.01	1.31	2.03	2.08	1.89	2.11	2.52	1.84	2.34	5.91	6.77	3.50
Al_2O_3	0.41	0.35	0.46	0.44	0.51	0.55	0.36	0.28	0.40	0.92	0.64	0.35
Fe_2O_3*	1.27	1.32	1.19	1.06	1.09	1.17	1.04	0.87	1.23	1.86	2.03	1.71
MnO	0.22	0.20	0.24	0.25	0.27	0.27	0.25	0.21	0.25	0.66	0.48	0.29
MgO	0.53	0.48	0.51	0.38	0.54	0.50	0.60	0.40	0.51	0.98	0.60	0.64
CaO	51.78	51.93	51.52	52.27	52.09	52.26	52.90	52.45	52.32	50.70	51.43	52.28
Na_2O	1.19	1.46	1.58	1.24	1.63	1.53	1.51	1.43	1.29	0.39	0.45	0.67
K_2O	0.26	0.22	0.17	0.19	0.20	0.29	0.19	0.18	0.18	0.40	0.26	0.58
P_2O_5	26.46	25.90	25.30	26.19	25.30	24.26	24.97	24.61	25.40	17.50	13.08	20.15
H_2O	3.08	2.41	2.06	2.65	2.85	2.38	2.14	3.02	2.66	3.16	2.87	2.21
CO_2	11.65	12.34	12.91	12.01	11.78	13.14	12.25	12.76	11.89	16.33	20.80	15.82
F	1.59	1.58	1.75	1.40	1.65	1.67	1.30	1.50	1.66	0.96	0.78	1.24
S	0.54	0.71	0.69	0.69	0.70	0.62	0.59	0.53	0.65	0.35	0.41	0.32
O = F	0.67	0.67	0.74	0.59	0.69	0.70	0.55	0.63	0.70	0.40	0.33	0.52
Total	100.32	99.55	99.67	100.26	99.81	100.05	100.07	99.45	100.08	99.97	100.17	99.24

Table 5
Content of some trace elements (ppm) in dinosaur bone remains

Elements	Vertebrae						Extremities						Skull			Pelvis			Ribs			Altered extremities		
	2V	4V	6V	8V	10V	12V	2E	4E	6E	8E	10E	12E	14E	2S	8S	12S	2P	8P	12P	2R	8R	12R	2Al	6Al	10Al
Sr	2400	2250	2060	2700	3100	3250	2340	2150	2000	2570	2850	2800	2950	2100	2500	2880	1900	2180	2600	1930	2150	2600	1580	1500	1980
Ba	825	790	710	1100	1200	1300	800	780	730	930	980	980	1050	810	920	950	685	790	890	650	710	830	1060	1100	750
Pb	138	130	117	153	152	158	124	120	120	135	130	144	157	126	118	130	112	105	126	96	94	108	74	85	91
La	1240	1160	1080	1400	1560	1640	1300	1150	1130	1600	1600	1650	1620	1250	1360	1530	1200	1280	1490	1100	1180	1350	765	700	1100
Ce	2750	2600	2490	2650	2600	2640	2700	2520	2520	2650	2600	2520	2500	1980	1900	1920	1880	1800	1800	1100	1000	1050	1650	1230	1710
Nd	1720	1530	1420	1600	1640	1600	1650	1480	1400	1310	1350	1290	1250	1300	1220	1100	1450	1280	1100	1100	970	810	870	630	900
Sm	550	510	480	650	720	710	525	450	460	460	490	520	520	420	450	500	400	460	470	230	300	320	255	200	350
Gd	370	350	330	440	415	470	340	250	250	280	310	320	305	300	320	385	275	300	300	200	265	290	385	140	220
Dy	550	500	500	650	725	715	515	440	480	480	540	530	530	350	385	460	520	630	645	340	430	490	250	210	380
Yb	80	73	75	110	106	103	83	73	74	95	95	98	97	76	100	105	73	96	103	60	82	100	44	41	67
Y	2290	2200	2080	3600	3780	3800	2200	2230	2100	2500	2500	2600	2680	2300	2450	2600	1990	2150	2470	1800	2070	2260	1300	1090	1700
Sr/Ba	2.9	2.8	2.9	2.5	2.6	2.5	2.9	2.8	2.7	2.8	2.9	2.9	2.8	2.6	2.7	3.0	2.8	2.8	2.9	3.0	3.0	3.1	1.5	1.4	2.6
La/Yb	16	16	14	13	15	16	16	16	15	17	17	17	17	16	14	15	16	13	14	18	14	14	17	17	16
LREE/HREE	6.3	6.3	6.0	5.3	5.2	5.1	6.6	7.3	6.9	7.0	6.4	6.3	6.3	6.8	6.1	5.3	5.7	4.7	4.6	5.9	4.4	4.0	5.2	7.1	6.1

remains buried at different times. Later remains are richer in silica, carbon dioxide, and fluorine relative to earlier remains (Table 4) in accordance with changes of the bone apatite composition (Table 3).

The bone remains are enriched in REE, Y, Sr, and Ba (Table 5; Fig.7). They contain up to 0.79% REE, up to 0.38% Y, up to 0.33% Sr, and up to 0.13% Ba. The REE spectrum is characterized by relative enrichment in LREE. The value of the LREE/HREE ratio is 4.0–7.3 with La/Yb = 13–18. Ce, La and Nd play a leading part among LREE and Dy –among HREE. The Gd/Dy ratio is 0.47–0.86. REE and Y are mainly concentrated in the phosphate fraction and partly in the carbonate fraction (Table 3). The bone remains are characterized by the prevalence of Sr relative to Ba with Sr/Ba = 2.5–3.1.

Some characteristic variations in trace element composition of the bone remains are noted; these are typical for all types of dinosaur bone remains. Vertebrae are characterized by the stratigraphically significant high–low–high oscillation of REE, Y, Sr, and Ba distribution (Fig.8).

The concentrations fall from bed 2 (sample 2V) to bed 6 (sample 6V) and then rise again to bed 12 (sample 12V). The same pattern is established for bone remains from extremities with the concentration maximum of REE, Y, Sr, and Ba for the uppermost redbed (bed 14) of the Maastrichtian sequence. For other types of bone remains data are incomplete. For skull, pelvis and ribs, there was a total enrichment in REE, Y, Sr, and Ba from bed 2 to bed 12, but their remains were not found in bed 6.

In parallel with the depletion of bones in REE, their relative enrichment in LREE is observed, with the increase of Ce/Y, La/Y, and Nd/Y ratios. Accordingly, Y > La, Ce, Nd and lowered values of the LREE/HREE ratio characterize the bone remains from the upper half of the studied section (Table 5).

Thus, there is a tendency towards enrichment in REE, Y, Sr, and Ba during the Maastrichtian up to the K/T boundary, typical for different types of bone remains. This tendency is complicated by some trace element depletion of bone remains within the lower part of the Maastrichtian sequence with the concentration minimum at bed N6.

6.3.2. Epigenetically altered remains

Chemical composition of epigenetically altered

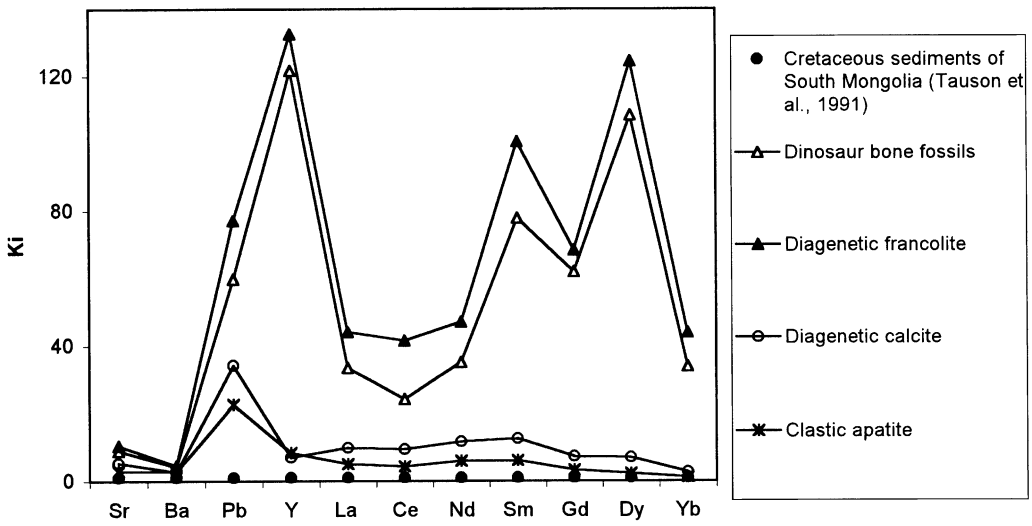

Fig. 7. Trace element abundances in dinosaur bone fossils, diagenetic francolite, diagenetic calcite, and clastic apatite, normalized to the average composition of Cretaceous sedimentary rocks of South Mongolia (Tauson et al., 1991).

remains is significantly distinguished from chemical composition of remains unaffected by this alteration. The depletion in phosphorus, fluorine, sulfur, and alkalis with some enrichment in calcium, carbon dioxide, as well as in silica, iron, and magnesium is characteristic for epigenetic alteration (Table 4). These changes are well correlated with the main mineralogical feature of epigenesis, mainly the calcitization of bone remains.

The altered bones can contain as little as 0.15% Sr, 0.11% Y, and 0.3% REE, significantly less than bone remains unaffected by epigenetic alteration (Table 5). Epigenetic processes did not mobilize barium, and accordingly, the Sr/Ba ratio decreases to 1.4. Epigenetic alteration led not only to total REE decrease, but also to the change of the REE spectrum. Altered bones are characterized by $Ce > La > Nd > Gd$ $Dy \sim Sm$ with $Ce > Y$. They have also higher LREE/HREE values.

6.4. Geochemical features of turtle remains

The turtle remains are also enriched in REE, Y, Sr, and Ba (Table 6). They contain up to 0.64% REE, up to 0.25% Y, up to 0.27% Sr, and up to 0.056% Ba. The REE spectrum is characterized by the significant prevalence of LREE. The value of the LREE/HREE ratio is 5.2–6.4 with $La/Yb = 15–23$. Ce, La and Nd play a leading part among LREE and Dy and Gd among HREE with $Dy > Gd$ ($Gd/Dy = 0.6–0.8$). The turtle remains are characterized by the significant prevalence of Sr relative to Ba with $Sr/Ba = 3.9–6.5$.

The remains found in uppermost part of the Maastrichtian sequence are most enriched in the considered trace elements, whereas late Paleocene remains are the most depleted. This is true for the turtle remains belonging to the same genus, *Mongoleums* (Tables 1 and 6) whose biostratigraphic range extends across the K/T boundary (Devyatkin, 1981). Maastrichtian and Paleocene turtle remains are also distinguished by their REE spectra. Maastrichtian remains are poorer in LREE relative to HREE and La relative to Yb, but are richer in Ba relative to Sr and Y relative to individual REE. Late Paleocene remains are characterized by the predominance of La, Ce, and Nd relative to Y and are characterized by Ce/Y, La/Y and $Nd/Y \geq 1$ (1.01–1.28), whereas these ratios are less than 1 (0.5–0.7) for Maastrichtian remains.

On the whole, carapace remains are characterized by a stratigraphically significant high–low–high–low oscillation of trace element concentrations (Fig. 9). The first maximum corresponds to earliest Maastrichtian sediments (bed 2, sample 2T) and the second

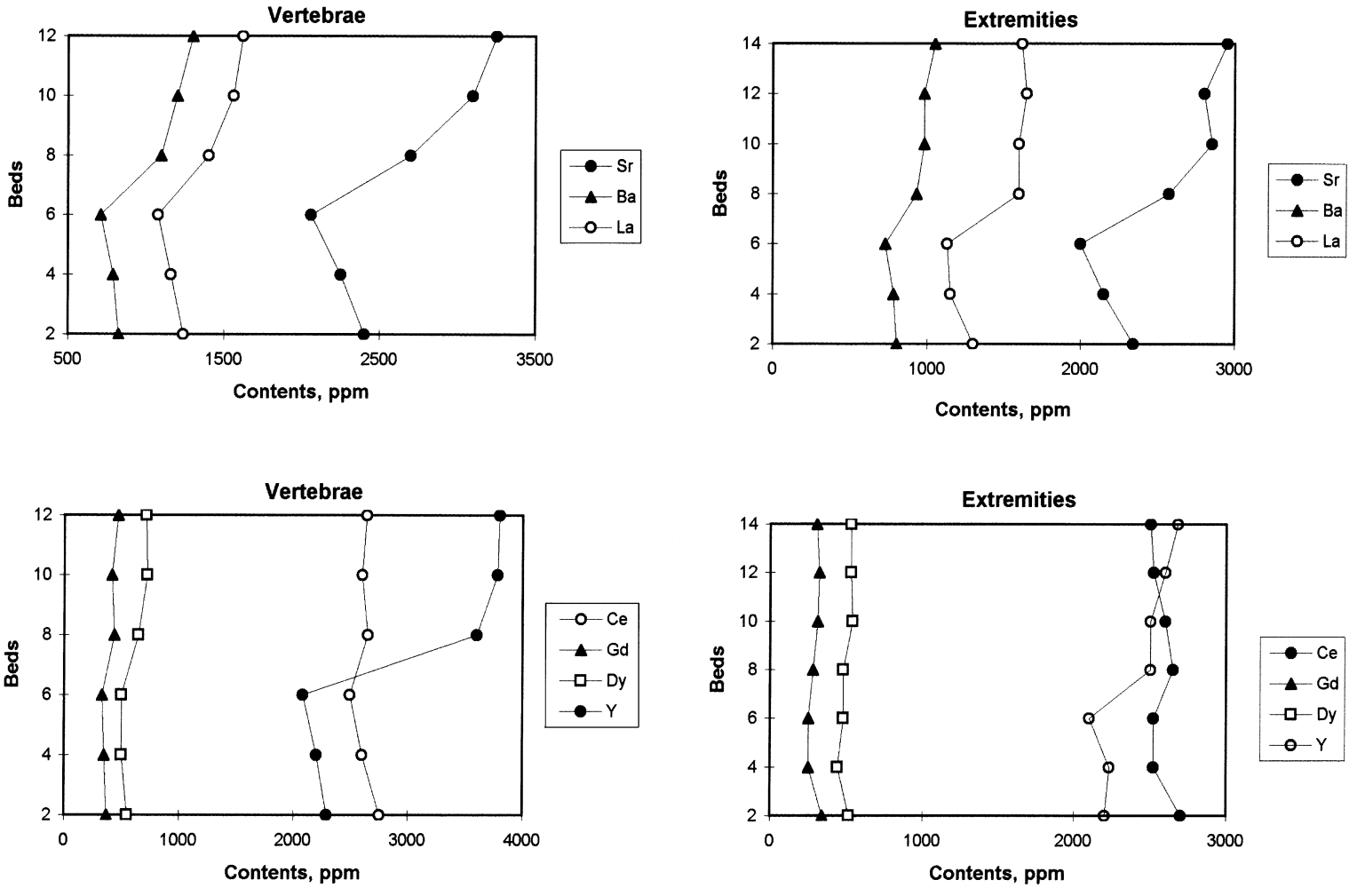

Fig. 8. Variation of the trace element composition of dinosaur bone fossils in the studied sequence.

Table 6
Contents of some trace elements (ppm) in turtle carapace remains (the Naran Bulak locality, South Mongolia)

	Maastrichtian remains							Paleocene remains		
Elements	2T[a]	4T	6T	8T	10T[a]	12T	14T	16T	17T[a]	18T
Sr	1950	1960	1800	2080	2300	2500	2650	1630	1600	1340
Ba	490	500	390	470	500	560	550	250	250	200
Pb	108	92	81	130	130	122	147	59	62	44
La	1200	1220	1130	1250	1450	1400	1510	850	850	750
Ce	1490	1330	1250	1460	1660	1650	1700	940	950	880
Nd	1350	1300	1200	1380	1370	1480	1590	850	830	770
Sm	370	400	300	410	400	480	520	230	200	175
Gd	280	250	240	250	300	325	360	205	190	144
Dy	380	350	300	440	450	450	580	215	200	198
Yb	70	73	70	75	83	91	90	36	35	29
Y	2250	2120	2000	2340	2300	2450	2410	840	800	690
Sr/Ba	4.1	3.9	4.6	4.4	4.6	4.5	4.8	6.5	6.4	6.7
LREE/HREE	6.0	6.3	6.4	5.9	5.9	5.8	5.2	6.3	6.7	6.9
La/Yb	17	17	16	17	17	15	17	24	24	26
Ce/Y	0.66	0.63	0.63	0.62	0.72	0.67	0.71	1.12	1.19	1.28
La/Y	0.53	0.58	0.57	0.53	0.63	0.57	0.63	1.01	1.06	1.09
Nd/Y	0.60	0.61	0.60	0.59	0.60	0.60	0.66	1.01	1.04	1.12

[a] The remains of *Mongoleums* sp.

maximum to latest Maastrichtian sediments (bed14, sample14T). The first minimum corresponds to the bed 6 (sample 6T) of earlier Maastrichtian and the second minimum to latest Paleocene sediments (bed18, sample18T). The greatest change in the accumulation of REE, Y, Sr, Ba is noted across the K/T boundary, from latest Maastrichtian to earliest Late Paleocene. At this boundary, the concentration maximum, and the following concentration minimum, are expressed more sharply than that for the earlier Maastrichtian.

Thus, the tendency towards change of geochemical features of turtle remains is expressed by special enrichment in REE, Y, Sr, and Ba in the uppermost part of the Maastrichtian section followed by significant depletion in the Paleocene. This tendency postdates a trace element depletion event in the lower part of the Maastrichtian sequence (Fig. 9).

7. Discussion

7.1. Climatic conditions of Maastrichtian sedimentation in the Naran Bulak region

Considerable variations are noted in mineral and chemical composition of Maastrichtian and Late Paleocene sediments, primarily of authigenic calcite, gypsum, and halite contents. The accumulation of these minerals in Maastrichtian–Late Paleocene sediments is evidence for development of aridity, and hence indicates paleoclimatic changes in Inner Asia from the Maastrichtian to the Paleocene.

The oscillating change of authigenic mineral contents in lacustrine and mudflow sediments corresponds to this climatic change. Lacustrine deposits bed N5 is especially depleted in authigenic minerals and, accordingly, in CO_2, SO_3, and Cl, whereas bed N15 are richest in these minerals and components (Table 2; Fig. 3). This indicates that deposition of the latest Maastrichtian lacustrine sediments of bed N15 took place in a particularly arid setting, whereas the arid minimum corresponds to the deposition of lacustrine bed N5.

Late Paleocene lacustrine sediments are characterized by clearly lower concentrations of CaO, CO_2, SO_3, and Cl, indicating again a progressive increase in humid conditions in the late Paleocene.

This same pattern of change of mineral and chemical composition of Maastrichtian sediments is well correlated also with the change of their thickness

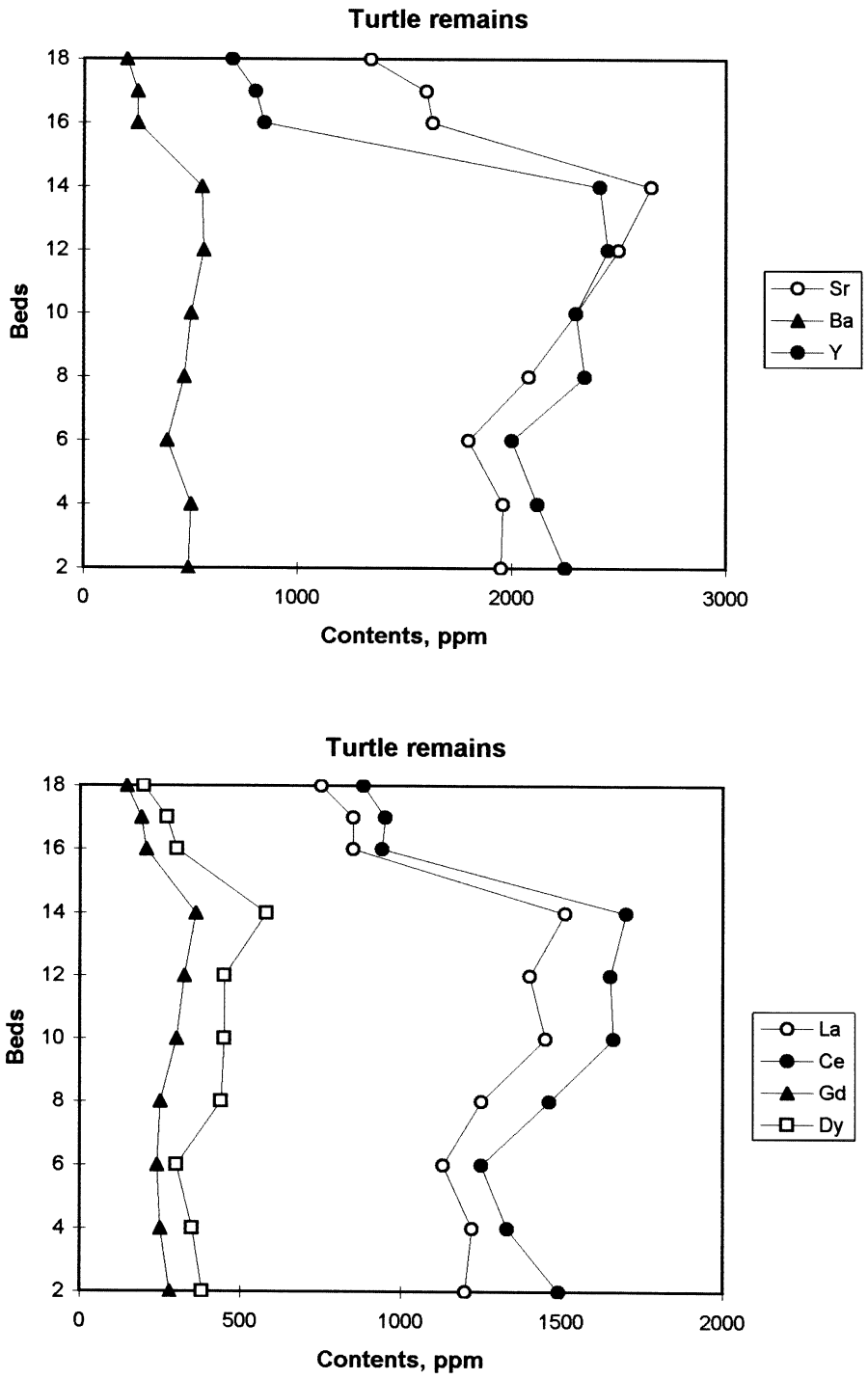

Fig. 9. Variation of the trace element composition of turtle carapace remains in the studied sequence.

and granulometric composition, but is oppositely directed in the studied sequence in accordance with the influence of aridity on the formation of these two sediment types. As aridity progresses, lacustrine deposit thickness decreases, as does the clay fraction within it, while silt and sand increases, as does the thickness of sandy–silty interbeds. This points to change of sedimentation conditions over this period. The period corresponding to the deposition of lacustrine bed N5 was characterized by particularly calm and deep conditions of the Maastrichtian lakes.

The end of the Maastrichtian is characterized by reduced rates of lake sedimentation bringing in less clay, in parallel with more intense storms bringing in coarse sediments and mudflows into an especially shallow setting.

Variations of redbed thicknesses may be considered as a function of the intensity of desert storm events that are climate-related, as increased aridity leads to the increase in energy of these individual events, accordingly forming thicker mudflows and their enrichment in authigenic minerals. Furthermore, fragments of Maastrichtian pedogenic deposits, formed in semiarid conditions, become more and better developed with increased redbed thickness, and are preserved in situ at the top of the Maastrichtian section, when the lake dried up entirely.

Thus, sedimentary rock lithology and chemistry shows that the Maastrichtian sediments were formed under conditions of increasing aridity. Lacustrine sedimentation was periodically interrupted by rainstorm events that led to the formation of mudflows, containing eroded sands and some pedogenic clasts. The transportation and resedimentation of these materials formed carbonate sandstone redbeds. These events become more prominent towards the end of the Maastrichtian leading up to the cessation of lacustrine sedimentation in this time.

A considerable role for sandstorm events in the southeastern part of the Gobi Basin was shown for the formation of the eolian sediments of Djadokhta Formation (Jerzykiewicz et al., 1993). It is also possible that in the studied area, not only desert rainstorm events, but also sandstorms are recorded. As aridity increased, sand and silt components were transported by the strong winds into the Maastrichtian lake. In our case, sandstorm events were not responsible for burial of vertebrate remains, however.

7.2. Genetic significance of the sediment geochemical features

Major and trace element compositions of the sedimentary rocks change in parallel. Clear positive correlation is noted between contents of REE, Y, Sr, and Ba, on the one hand, and CaO, CO_2, SO_3, and Cl, on the other hand (Table 2; Fig. 3). These data point to the leading role of sedimentation processes as responsible for geochemical features in the lacustrine and mudflow deposits.

Authigenic calcite was the main sink for the trace elements, as the increase in its content is accompanied by a rise of the trace element concentrations. The calcite content both in lacustrine sediments and in redbeds is related to aridity, which controlled the salinity regime of sedimentation in the lakes. Accordingly, there is a relationship between aridity and the trace element composition of sedimentary rocks enclosing the vertebrate remains.

The increase in REE, Y, Sr, and Ba contents correlates with relative aridization, whereas their decrease correlates with return to humid conditions. The maxima and minima of trace element concentrations are correlated with the maxima and minima of relative aridization as outlined above. The latest Maastrichtian sediments that are richest in REE, Y, Sr, and Ba correspond to the maximum of aridization at the K/T boundary (Fig. 3). Earlier Maastrichtian and late Paleocene sediments formed under more humid conditions are depleted in trace elements.

Thus, aridization was very important factor regulating the concentration levels for REE, Y, Sr, and Ba in the sediments. Accordingly, trace element composition of the studied sediments can be also considered as an indicator of paleoclimatic changes at the K/T boundary in the Gobi Desert.

7.3. The possible origin of trace elements in vertebrate bone remains

The important features of the studied bone remains are: (a) the excellent textural preservation, mainly with the concentric texture that is the petrographical expression of modern bone osteons; (b) the enrichment in some trace elements, primarily in REE, Y, and Sr; and (c) oscillatory distribution pattern of these trace elements in the section. These features

were formed after sedimentation, but before post-fossilization epigenetic processes, at the early diagenesis stage of the buried bone remains.

Bone tissue of living vertebrates is composed of an organic matrix. The space between this matrix is impregnated with biominerals, among which the hydroxyl variety of apatite plays a dominant role. Compact bone consists of apatite lamellae arranged concentrically around an osteonal canal, or rarely, in periosteal bone in flat sheets. The osteonal canal and its surrounding mineral lamellae constitute an osteon. The apatite crystalline aggregates comprise numerous elongate cavities (lacunae) and interconnecting canals (canaliculi) filled with interstitial fluid that is rich in non-crystalline phosphorus. The dynamic equilibrium between crystalline apatite and interstitial fluid regulates the chemical and salt balance in bone tissue, and to some extent, in the entire organism. Apatite serves as a chemical depot for many elements, including some with potentially unfavorable effects on living vertebrates (Martill, 1991; Kent, 1992).

The studied fossilized dinosaur remains are in fact pseudomorphs after buried living dinosaur bones (Kolodny et al., 1996). The fossilized remains reflect living bone structure characterized by osteonal texture although it has not been recorded in all dinosaurs. Diagenetic fossilization involves complete mineralization of these dinosaur bones with the crystallization of calcite–francolite aggregates. This replacement of bone apatite by francolite took place together with deposition of diagenetic calcite following the removal in solution of degraded organic tissues.

The factor that was favorable for this exceptional preservation of bone textural features was the rapid burial of the dinosaur remains. In the Naran Bulak locality, there is a direct relationship between the type of sedimentation and preservation of faunal remains. Lacustrine sedimentation was periodically interrupted by mudflows due to relatively powerful, short acting torrents, typical for arid areas. Death and rapid burial of vertebrate faunas accompanied these mudflows. The sediment mass containing the buried skeletons was sealed into the relatively impermeable lake bottom sediments and protected against rapid oxidation and destruction by scavengers.

The most striking feature of preservation of the faunal remains in the Naran Bulak locality was the relatively slight degree of postfossilization epigenesis. The latter process, when occurred, led to the destruction of concentric bone texture and the dissolution of their apatite framework.

Trace element enrichment of reptile remains took place during diagenesis of the buried remains under the influence of pore waters. The importance of chemical changes of faunal remains during this stage has been shown by investigations of different vertebrates, including dinosaur remains (McArthur and Walsh, 1984/1985; Elderfield and Pagett, 1986; Grandjean et al., 1987, 1998; Piper, 1991; Schmitz et al., 1991; Wright et al., 1987; Trueman, 1996; Samoilov and Benjamini, 1996).

Trace elements including REE were mainly concentrated in diagenetic francolite. Diagenetic calcite played a lesser role in the concentration of the trace elements. The preferential trace element concentration in bone francolite was related to higher isomorphic potential of apatite for many chemical elements, both for cations and anions. However, this potential was not realized for clastic apatite from the same sedimentary rocks that include the enriched bone remains. This difference may be attributed to the more significant surface of interaction with pore waters for buried bones than for clastic apatite. However, this difference would not have been so great between interaction surfaces of diagenetic bone calcite and sedimentary authigenic calcite. The latter forms numerous small grains composing up to 35% of redbed volume, but is considerably poorer in REE, Y, and Sr than calcite of fossilized bones (Table 3).

In our opinion, the observed difference in the trace element composition of bone- and rock-forming minerals can be attributed to the presence of original organic material in buried bones. Such degraded organic material attached to buried vertebrate bones was the favorable geochemical barrier enabling trace element accumulation in fossilized bones.

Geochemical barriers are characterized by sharp decrease of element mobility together with the formation of geochemical anomalies. For example, buried bones enriched in degraded organic material had significant influence on redox potential of the bone-pore water system, resulting in the precipitation of some components of these water solutions in the buried bones during their mineralization. Trace element accumulation in the fossils then ceased after

the complete degradation of organic material, in spite of the very prolonged subsequent interaction of these fossils with pore waters. Considerably later interactions with pore waters led in fact to destruction of bone structure, dissolution of apatite, and subtraction of REE, Y, and Sr.

The considerable enrichment in some trace elements, especially in REE is very typical for vertebrate bone fossils independently of the environmental conditions of their burial. The REE content is extremely low in living bones of marine or terrestrial vertebrates, from small fish bones up to large dinosaur bones, but they are considerably enriched in REE after their burial.

In the studied sequence, positive correlation is noted between the distribution patterns of trace elements for vertebrate bone fossils and their enclosing redbeds (Figs. 3, 8, and 9). They are characterized by similar pattern of change and identical trace element maxima and minima. These changes reflect first humid, then arid, and again humid conditions from the Maastrichtian to the late Paleocene.

Thus, trace element composition of the vertebrate fossils is a trace of Maastrichtian–Late Paleocene paleoclimate. The cause was an influence of the composition of interacting pore water on fossilized bone chemistry. Aridity development led to the increase in pore water salinity favorable for the trace element accumulation in the crystallized minerals. In any case, the length of time between death of the reptiles and the complete early diagenetic fossilization of their remains was much shorter than the time scale of climatic change.

The rate of diagenetic fossilization depends on preservation potential of bone organic constituents. Nucleic acids are degraded by hydrolysis and have the lowest preservation potential. Lipids are more stable relative to other biomolecules of animals, but biolipids transform to geolipids with considerable structural alteration. Proteins are variably stable in buried conditions and their insignificant quantities can be sometimes found as intracrystalline inclusions in diagenetic apatite. In relation to the rate of diagenetic fossilization of large terrestrial vertebrate bones, degradation rate of such proteins as osteocalcin, skeletal glycoproteins and especially collagen, which form a considerable part of the vertebrate bones, is of significance.

Other factors being equal, the composition of the waters interacting with burial bones has considerable influence on the rate of diagenetic mineralization of burial bones. The length of diagenesis is bound to be shorter if it is affected under the influence of water sources with high salinity, such as indicated by the climatic conditions of the studied setting.

8. Conclusions

The Maastrichtian dinosaur bones of the Naran Bulak locality (South Mongolia) display the concentric texture pseudomorphic after the osteonal bone texture of living animals. Factors favorable for the preservation of bones and their textural features are rapid burial and relatively limited subsequent epigenetic destruction. The rapid burial of the bones was a result of violent mudflow events of powerful, short-acting torrents, typical for arid areas. Such burial in mudflow deposits within the lacustrine environmentprovides an effective sealing process.

Diagenetic alteration of the dinosaur bones was expressed as complete mineralization, with crystallization mainly of francolite–calcite aggregates. Francolite replaced biological hydroxyl-apatite and part of the organic matter between haversian canals, and calcite replaced only organic matter of the haversian canals.

Trace element enrichment and textural preservation of reptile remains occurred during diagenesis under the influence of pore waters, interacting with degrading bone organic material.

All types of dinosaur and turtle bone remains from the Naran Bulak locality are enriched in REE, Y, Sr, and Ba. Trace elements including REE were mainly concentrated into diagenetic Françoise with diagenetic calcite playing a lesser role. The maximum trace element accumulation took place near the top of the Maastrichtian. Paleocene turtle remains are successively less enriched in REE, Y, Sr, and Ba above the K/T boundary.

Maastrichtian sediments were formed under changing climatic conditions with progressive aridity development towards the K/T boundary. This process led to drying up of the lake at the end of the Maastrichtian. As aridity progressed, lacustrine sedimentation was periodically interrupted by mudflows caused by rainstorm events, and the formation of redbeds with trapped preserved vertebrate remains.

Increase in aridity was the most important factor regulating the concentration levels for REE, Y, Sr, and Ba in the sediments. The trace element accumulation in the sediments is well correlated with the aridity rise and shows the aridity maximum near the K/T boundary. The latest Maastrichtian sediments are richest in REE, Y, Sr, and Ba and represent especially arid conditions, whereas earlier Maastrichtian rocks and later Paleocene sediments are poorer in them and were formed under humid conditions.

There is a positive correlation between REE, Y, Sr, and Ba and CaO, CO_2, SO_3, and Cl concentrations both in the sediments and reptile bone remains. Thus, change in chemical composition not only for sediments, but also for faunal remains, is compatible with the paleoclimatic changes in Inner Asia towards the K/T boundary. The change of the bone trace element composition is also correlated with progressive aridization towards the top of the Maastrichtian.

On the whole, our data show the following:

1. Trace element enrichment of the reptile remains occurred at the time of early diagenetic mineralization, with the neoformation of mineral calcite–francolite aggregates.
2. Chemical composition of the studied sediments was formed under Maastrichtian–Late Paleocene climatic settings characterized by increasing aridity towards the K/T boundary.
3. The trace element composition of reptile remains is also compatible with the same paleoclimatic changes in Inner Asia, indicating that the length of time between death of the reptiles and early diagenetic stabilization of trace elements in their remains is reasonably shorter than the rate of climatic changes.
4. The composition of the pore water played an important role in the bone trace element enrichment. The increase of water salinity as a function of aridity led to more effective concentration of trace elements both in the buried reptile remains and in sediments enclosing them.

Acknowledgements

The authors are thankful to Dr V.F. Shuvalov (Institute of Limnology, St Petersburg, Russia) for consultations in paleontology and stratigraphy, and to S. Shigarova and S. Yaroshenko (Vinogradov Institute of Geochemistry, Irkutsk, Russia) for their help in the analytical investigations. Criticism by the 'Sedimentary Geology' reviewers resulted in a more balanced presentation of the manuscript.

References

Ayliffe, L.K., Lister, A.M., Chivas, A.R., 1992. The preservation of glacial–interglacial climatic signatures in the oxygen isotopes from elephant skeletal phosphate. Palaeogeogr., Palaeoclimatol., Palaeoecol. 99, 179–191.

Barrick, R.E., Showers, W.J., 1994. Thermophysiology of *Tyrannosaurus rex*: evidence from oxygen isotopes. Science 265, 222–224.

Barsbold, R., 1972. Late Cretaceous Biostratigraphy and Limitic Mollusks in Gobian Part of Mongolian People Republic. Nauka, Moscow (in Russian).

Bocherens, H., Fizet, M., Mariotti, A., 1994. Diet, physiology and ecology of fossil mammals as inferred by stable carbon and nitrogen isotopes biochemistry: implications for Pleistocene bears. Palaeogeogr. Palaeoclimatol. Palaeoecol. 107, 213–225.

Bryant, J.D., Luz, B., Froelich, P.N., 1994. Oxygen isotopic composition of fossil horse tooth phosphate as a record of continental paleoclimate. Palaeogeogr., Palaeoclimatol., Palaeoecol. 107, 303–316.

Deer, W.A., Howie, R.A., Zusman, J., 1965. Rock-forming Minerals. Longmans, London.

Devyatkin, E.V., 1981. Cenozoic in Inner Asia. Nauka, Moscow.

Devyatkin, E.V., Shuvalov, V.F., 1980. Continental Mesozoic and Cenozoic of Mongolia (stratigraphy, geochronology, paleogeography). In: Zaitzev, N.S., Kovalenko, V.I. (Eds.), Evolution of Geological Processes and Metallogenesis of Mongolia. pp. 165–176 (in Russian).

Downing, K.F., Park, L.E., 1998. Geochemistry and early diagenesis of mammal-bearing concretions from the Sucker Creek Formation (Miocene) of southeastern Oregon. Palaios 13 (1), 14–27.

Elderfield, H., Pagett, R., 1986. Rare-earth elements in ichthyolites: variations with redox conditions and depositional environment. The Science of the Total Environment 49, 175–197.

Gile, L.H., Hawley, J.W., Grossman, R.B., 1981. Soil and geomorphology in a basin and range area of southern New Mexico. Guidebook to the Desert Project, New Mexico Bureau of Mine and Mineral Resources. Memoir 39, pp. 1–222.

Gradzinski, R., Kielan-Jaworowska, Z., Maryanska, T., 1977. Upper Cretaceous Djadokhta, Barun Goyot and Nemegt formations of Mongolia, including remarks on previous subdivisions. Acta Geologica Polonica 27, 281–318.

Grandjean, P.H., Albarede, F., 1989. Ion probe measurements of rare earth elements in biogenic phosphates. Geochim. Cosmochim. Acta 53, 3179–3183.

Grandjean, P.H., Capetta, H., Michard, A., Albarede, F., 1987. The

assessment of REE patterns and $^{143}Nd/^{144}Nd$ ratios in fish remains. Earth and Planetary Science Letters 84, 181–186.

Grandjean, P.H., Capetta, H., Albarede, F., 1988. The REE and Nd of 40–70 Ma old fish debris from the West-African platform. Geophysical Research Letters 15 (4), 389–394.

Grandjean, P., Feist, R., Albarede, F., 1993. Significance of rare element in old biogenic apatites. Geochim. Cosmochim. Acta 57, 2507–2514.

Hubert, J.F., Panish, P.T., Chure, D.J., Prostak, K.S., 1996. Chemistry, microstructure, petrology, and diagenetic model of Jurassic dinosaur bones, Dinosaur National Monument, Utah. J. Sediment. Res. 66, 531–547.

Jerzykiewicz, T., Currie, P.J., Eberth, D.A., Johnston, P.A., Koster, E.H., Zheng, J., 1993. Djadokhta Formation correlative strata in Chinese Inner Mongolia: an overview of the stratigraphy, sedimentary geology, and paleontology and comparisons with the type locality in the pre-Altai Gobi. Can. J. Earth Sci. 30, 2180–2195.

Jerzykiewicz, T., 1998. Okavango Oasis, Kalahari Desert: A contemporary analogue for the late Cretaceous vertebrate habit of the Gobi Basin, Mongolia. Geoscience Canada 25 (1), 15–26.

Kent, G.C., 1992. Comparative anatomy of the vertebrates. Mosby Year Book.

Kielan-Jaworowska, Z., 1969. Hunting for Dinosaurs. MIT Press, Cambridge (Mass).

Kolodny, Y., 1983. In: Emiliani, C. (Ed.), Phosphorites. The Sea, vol. 7, pp. 981–1023.

Kolodny, Y., Luz, B., 1992. Isotope signatures in phosphate deposits: formation and diagenetic history. In: Clauer, H., Chaudhuri, S. (Eds.), Isotopic Signatures and Sedimentary Records. Springer Verlag, Berlin, pp. 69–122.

Kolodny, Y., Luz, B., Sander, M., Clemens, W.A., 1996. Dinosaur bone: fossil or pseudomorphs? The pitfalls of physiology reconstruction from apatitic fossils. Palaeogeogr., Palaeoclimatol., Palaeoecol., 126 (1–2), 161–171.

Lee-Thorp, J.A., Vander Merwe, N.J., 1991. Aspects of the chemistry of modern and fossil biological apatite. J. Archeol. Sci. 18, 43–354.

Longinelli, A., 1984. Oxygen isotopes in mammal bone phosphate: A new tool for paleohydrological and paleoclimatological research? Geochim. Cosmochim. Acta 48, 385–390.

Luz, B., Kolodny, Y., 1985. Oxygen isotope variation in phosphate of biogenic apatites, IV. Mammal teeth and bones. Earth Planet. Sci. Lett. 75, 29–36.

Luz, B., Kolodny, Y., 1989. Oxygen isotope variation in bone phosphate. Appl. Geochem. 4, 317–323.

Luz, B., Kolodny, Y., Horowitz, M., 1984. Fractionation of oxygen isotopes between mammalian bone phosphate and environmental drinking water. Geochim. Cosmochim. Acta 48, 1689–1693.

Luz, B., Cormie, A.B., Schwarcz, H.P., 1990. Oxygen isotope variation in phosphate of deer bones. Geochim. Cosmochim. Acta 54, 1723–1728.

Martill, D.M., 1991. Bones as stones: the contribution of vertebrate remains to the lithologic record. In: Donovan, S.K. (Ed.), The Processes of Fossilization. Columbia Univ. Press, New York, pp. 270–292.

Martinson, G.G., 1975. The principles of stratigraphy and correlation of Mesozoic continental deposits of Mongolia. In: Martinson, G.G. (Ed.), Stratigraphy of Mesozoic Deposits of Mongolia. Nauka, Moscow, pp. 7–25 (in Russian).

McArthur, J.M., Walsh, J.N., 1984/1985. Rare-earth geochemistry of phosphorites. Chem. Geol. 47, 191–220.

Newesley, H., 1989. Fossil bone apatite. Applied. Geochem. 4, 233–245.

Person, A., Bocherens, H., Mariotti, A., Renard, M., 1996. Diagenetic evolution and experimental heating of bone phosphate. Palaeogeogr., Palaeoclimatol., Palaeoecol. 126 (1–2), 135–149.

Piper, D.Z., 1991. Geochemistry of a Tertiary sedimentary phosphate deposit: Baja California Sur, Mexico. Chem. Geol. 92, 283–316.

Rozhdestvensky, A.K., Tatarinov, L.P., 1964. Fundamentals of Paleontology: Amphibians, Reptiles and Birds. Nauka, Moscow.

Samoilov, V.S., 1984. Geochemistry of Carbonatites. Nauka, Mosco (in Russian).

Samoilov, V.S., 1989. Late Mesozoic rift magmatism in South Mongolia. Geology and Geophysics 9, 12–21.

Samoilov, V.S., Kovalenko, V.I., 1993. Complexes of Alkaline Rocks and Carbonatites of Mongolia. Nauka, Moscow.

Samoilov, V.S., Benjamini, Ch., 1996. Geochemical features of dinosaur remains from the Gobi Desert, South Mongolia. Palaios 11, 519–531.

Sanchez Chillon, B., Alberdi, M.T., Leone, G., Bonadonna, F.P., Stenni, B., Longinelli, A., 1994. Oxygen isotopic composition of fossil equid tooth and bone phosphate: an archive of difficult interpretation. Palaeogeogr., Palaeoclimat., Palaeoecol. 107, 317–328.

Schmitz, B., Aberg, G., Werdelin, L., Forey, P., Bendix-Almgreen, S.E., 1991. 87Sr/86Sr, Na, F, Sr and La in skeletal fish debris as a measure of the paleosalinity of fossil-fish habitats. Geol. Soc. Amer. Bull. 103, 786–794.

Shuvalov, V.F., 1982. Paleogeography and history of Mongolian lake system in Jurassic and Cretaceous. In: Martinson, G.G. (Ed.), Mesozoic Lake Basins of Mongolia. Nauka, Leningrad, pp. 18–80 (in Russian).

Tauson, L.V., Barsbold, R., Samoilov, V.S., Smirnova, E.V., Korytov, F., 1984. Trace elements in dinosaur remains from Gobian part of Mongolia. Dokl. Akad. Nauk SSSR 278 (4), 974–978 (in Russian).

Tauson, L.V., Samoilov, V.S., Barsbold, R., Shuvalov, V.F., 1990. Features of trace element composition of dinosaur remains from Mongolia. Dokl. Akad. Nauk SSSR 311 (1), 200–204 (in Russian).

Tauson, L.V., Samoilov, V.S., Smirnova, E.V., 1991. Rare earth elements in the dinosaur remains from Gobi desert. Geokhimia 4, 515–526 (in Russian).

Trueman, C.N., 1996. Variation of REE patterns in dinosaur bones from Northwest Montana: Implications for taphonomy and preservation. Geoscientist 6 (6), 27–30.

Trueman, C.N., 1999. Rare earth element geochemistry and taphonomy of terrestrial vertebrate assemblages. Palaios 14, 555–568.

Wang, Y., Cerling, T.E., 1994. A model of fossil tooth and bone

diagenesis: implications for paleodiet reconstruction from stable isotopes. Palaeogeogr., Palaeoclim., Palaeoecol. 107, 281–289.

Williams, C.T., 1988. Alteration of chemical composition of fossil bone by soil processes and groundwater. In: Grupe, G., Herrman, B. (Eds.), Trace Elements in Environmental History. Springer-Verlag, Amsterdam, pp. 27–40.

Wright, J., Schreder, H., Holser, W.T., 1987. Paleoredox variations in ancient oceans recorded by rare earths in fossil apatite. Geochim. Cosmochim. Acta 51, 631–644.